Low-pressure phase transformation from rhombohedral to cubic BN: Experiment and theory

Valery I. Levitas[1,*] and Leonid K. Shvedov[2]
[1]*Texas Tech University, Department of Mechanical Engineering, Lubbock, Texas 79409-1021*
[2]*V. Bakul Institute for Superhard Materials of the National Academy of Sciences of Ukraine, Kiev, Ukraine*
(Received 18 October 2000; revised manuscript received 3 October 2001; published 28 February 2002)

An irreversible phase transformation (PT) from the rhombohedral phase of boron nitride rBN to cubic cBN was recently recorded at the surprisingly low pressure of 5.6 GPa at room temperature. In this paper, a very nontrivial and unexpected explanation of this phenomenon is found, based on our criterion for the PT in plastic materials and approximate solution of corresponding plastic problems. It is found that due to orientational plastic instability and rotational softening in rBN and the higher yield stress of cBN, stresses grow drastically in the transforming region during the PT (despite a volume decrease by a factor of 1.53). This allows the fulfillment of the PT criterion which takes into account the whole stress history during the transformation process. It appears that the above experimental phenomenon is connected to the mechanical behavior of the system of transforming particles+surrounding materials at the millimeter scale.

DOI: 10.1103/PhysRevB.65.104109 PACS number(s): 64.60.−i, 64.70.Kb, 46.35.+z

I. INTRODUCTION

An irreversible phase transformation (PT) from the rhombohedral phase of boron nitride rBN to cubic (diamondlike) cBN was recorded at the pressure of 5.6 GPa and nonhydrostatic conditions.[1] That is one order of magnitude below the pressure of an irreversible transformation, 55 GPa, under the conditions of hydrostatic compression.[2] However, an explanation of this phenomenon was lacking. At the same time, a proper understanding of the reasons of the PT pressure reduction and underlying phenomena will allow us to purposefully use them for further reduction of the PT pressure, for finding material systems where a similar reduction can be expected, for a search of new superhard phases, and for application of these phenomena in engineering practice. The goals of this paper are to describe and interpret the PT observed in Ref. 1 and to obtain some additional experimental data necessary to check our theory.

Vectors and tensors are denoted in boldface type; $\mathbf{A}\cdot\mathbf{B}=(A_{ij}B_{jk})$ and $\mathbf{A}:\mathbf{B}=A_{ij}B_{ji}$ are the contraction of tensors over one and two nearest indices. A superscript -1 denotes inverse operation, $:=$ means equals per definition, subscript s designates symmetrization of the tensors, and the indices 1 and 2 denote the values before and after the PT.

II. EXPERIMENTAL RESULTS

We describe the experimental results obtained in Ref. 1 and our additional experiments, which are necessary to verify our theory. A very high-textured rhombohedral phase of BN, with disorientation of the C axes of crystallites about 3° with respect to the [0001] rBN texture axis, was compressed in diamond anvils along the [0001] rBN direction. Disk-shaped samples of a pyrolytic material containing up to 95 mass% rBN, 3 mm in diameter, were used. The ruby fluorescence technique was used to measure pressure in the center of the sample.[3] The basic difficulty consisted in the registration of ruby fluorescence spectra ($l=0.6942$ μm) because rBN has a strong luminescence in this spectral range. By choosing both the laser beam diameter and ruby chip dimensions (3.5 μm), we recorded sharp ruby fluorescence spectra. A detailed description of the diamond anvil cell and the measurement technique can be found in Ref. 4.

Up to about 3.5 GPa, the material was deformed elastically, because on unloading there was practically no anvil indent on the sample surface. At recompression in a range 4.2–5.6 GPa, small strips of 10×80 μm^2 size, well visible in transmitted light, appeared on the sample surface. In Ref. 1, these strips were interpreted as cracks; however, there was no crack evidence at unloading. Now we believe that a reorientation of crystallites under applied load takes place and these strips represent the boundary between differently oriented crystal regions.

When the pressure reached 5.6 GPa and the load was fixed, an amount of chaotically located strips increased quickly. After 5–7 s, an abrupt irreversible martensitic PT from rhombohedral rBN to cubic cBN was recorded at the sample center, accompanied by a distinct acoustic emission signal, significant reduction of the disk thickness, and dynamic loading.

The as-recovered sample of the produced bulk material looked like a plate of black color with mirror-smooth plane-parallel surfaces (Fig. 1). When the anvils were aligned well, the shape of the transforming region was close to a circle. The microhardness of the transformed material defined by Knoop microindentation was 49.6 GPa, which is typical of cBN. The analysis of electron-diffraction patterns of spalled particles of the sample uniquely shows the presence of a fair quantity of cBN. All measured geometric parameters of compressed disk and pressure at the beginning of the PT for several experiments are summarized in Table I. Parameters given in brackets were used in our calculations. Experiment No. 3, which corresponds to the small initial disk thickness, was accompanied by the spalling of a nonloaded disk part (at a radius greater than the anvil radius R). In experiment No. 4, one of the anvils received a ring crack. Its position approximately corresponds to the boundary between rBN and cBN phases. This anvil was polished to remove the crack. However, in the next experiment, after dynamic loading during the PT from rBN to cBN, it was broken into dust.

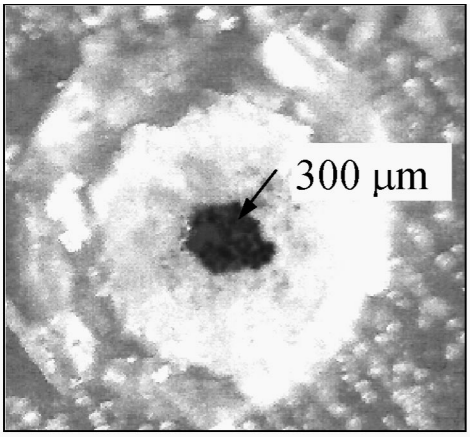

FIG. 1. View of the sample at the diamond anvils. Black region represents cBN transformed from rBN at the pressure 5.6 GPa at the beginning of the transformation.

III. PHASE TRANSFORMATION CRITERION

Recently a new general continuum thermodynamic and kinetic theory of the PT in elastoplastic materials was developed.[5–7] We will use only the equations we need for our study.

For a martensitic PT, the transformation deformation gradient $\mathbf{F}_t$ (Bain strain) transforms a crystal lattice of the parent phase into a crystal lattice of the product phase. As the behavior of inelastic materials is history dependent, consideration of the entire process of the growth of transformation deformation gradient $\mathbf{F}_t$ from unit tensor $\mathbf{I}$ to the final value $\mathbf{F}_{t2}$ in the transforming region is necessary. Transformation of a crystal lattice at PT rBN→cBN consists of 1.596-fold compression in the [0001] direction and an extension by a factor of 1.02 in the basal plane (orthogonal direction). Consequently, three principal values of the transformation deformation gradient $\mathbf{F}_{t2}$ are $F^z_{t2}=1/1.596=0.627$ and $F^r_{t2}=F^\theta_{t2}=1.02$. In the simplest case, when the temperature is fixed and homogeneous in a transforming volume and elastic strains are small, our thermodynamic criterion for a PT in the region with a mass m_n looks as follows:

$$X:=\frac{1}{m_n}\int_{m_n}\int_{\mathbf{I}}^{\mathbf{F}_{t2}}\frac{1}{\rho}\mathbf{T}:(d\mathbf{F}_t\cdot\mathbf{F}_t^{-1})dm_n - \frac{1}{2m_n}\int_{m_n}\int_{\mathbf{E}_1}^{\mathbf{E}_2}\frac{1}{\rho}\boldsymbol{\varepsilon}_e:d\mathbf{E}:\boldsymbol{\varepsilon}_e dm_n-\Delta\psi^\theta(\theta)=K. \quad (1)$$

TABLE I. Measured geometric parameters of compressed disk and axial stresses at the beginning of the PT.

	Radius of anvil, R (μm)	Radius of cBN phase, r_0 (μm)	Final thickness h (μm)	PT start pressure σ_{zi} (GPa)	Initial thickness h_i (μm)
1	250	100	26	5.6	310
2	375	~150	~50	~5.6	~450
3	375	70–105 (70)	~20	>5 (5.6)	~175
4	375	100–160 (100)	30–35 (30)	~5.5	380

Here X is the driving force for the PT, which represents the total calculated dissipation increment due to the PT only (i.e., excluding all other types of dissipation, e.g., plastic dissipation) during the entire transformation process, averaged over the transforming region; $\mathbf{T}$ is the true Cauchy stress, ρ is the variable mass density during the PT; $\mathbf{E}$ is the tensor of elastic moduli; $\boldsymbol{\varepsilon}_e$ is the elastic strain; $\Delta\psi^\theta$ is the jump in the thermal part of the Helmholtz free energy, θ is the temperature, and K is the experimental value of dissipation due to the PT. The key point of criterion (1) is that it takes into account the whole history of stress variation during the transformation process, which depends, in particular, on the interaction of the transforming region with the surrounding material. This may explain that the PT pressure obtained not only in different high-pressure apparatuses, but in the same apparatus under different conditions (e.g., geometry and properties of a gasket), differs significantly. Another important point is that the PT criterion (1) takes into account the stress tensor rather than the pressure only. For elastic materials, the expression for X coincides with the change in Gibbs free energy of the whole system per unit mass,[6] i.e., like in a standard approach.

When all parameters are homogeneously distributed in the transforming region and the stress tensor reduces to hydrostatic pressure p, $\mathbf{T}=p\mathbf{I}$, then using known kinematic relations[8] we obtain

$$\frac{1}{\rho}\mathbf{T}:(d\mathbf{F}_t\cdot\mathbf{F}_t^{-1})=\frac{p}{\rho}d\mathbf{F}_t:\mathbf{F}_t^{-1}=\frac{p}{\rho}d\ln\frac{\rho_1}{\rho}=pd\frac{1}{\rho}=\frac{1}{m}pdV=\frac{1}{\rho_1}pd\frac{V}{V_1},$$

where m is the mass of a small transforming particle, and V_1 and V are its volume before and during the PT. If pressure and elastic strains are fixed during the PT, Eq. (1) can be transformed into the form

$$\rho_1 X=p\left|\frac{V_2}{V_1}-1\right|-\frac{1}{2}\boldsymbol{\varepsilon}_e:\left(\frac{\rho_1}{\rho_2}\mathbf{E}_2-\mathbf{E}_1\right):\boldsymbol{\varepsilon}_e-\rho_1\Delta\psi^\theta(\theta)=\rho_1 K. \quad (2)$$

Here and later, we take the modulus of strains in order to consider compressive stresses (pressure) to be positive. If $K=0$, Eq. (2) describes the standard equilibrium line $p(\theta)$, which can be expressed as $p=A+B\theta$ with $A=-6.5$ GPa, $B=0.003\,54$ GPa/K.[9] Comparison of these two equations allows us to express two last terms in the expression for X through known material parameters. Then Eq. (2) can be transformed to

$$\rho_1 X=\frac{\rho_1}{m_n}\int_{m_n}\int_{\mathbf{I}}^{\mathbf{F}_{t2}}\frac{1}{\rho}\mathbf{T}:(d\mathbf{F}_t\cdot\mathbf{F}_t^{-1})dm_n-a-b\theta=\rho_1 K, \quad (3)$$

with $a=A|V_2/V_1-1|=-4.24$ GPa and $b=B|V_2/V_1-1|=0.002\,31$ GPa/K. At $K\neq 0$ we are able to describe the deviation of actual transformation lines for direct and reverse PT's from the equilibrium one, i.e., the pressure hysteresis. There are a lot of sources of dissipation K due to the PT (Ref.

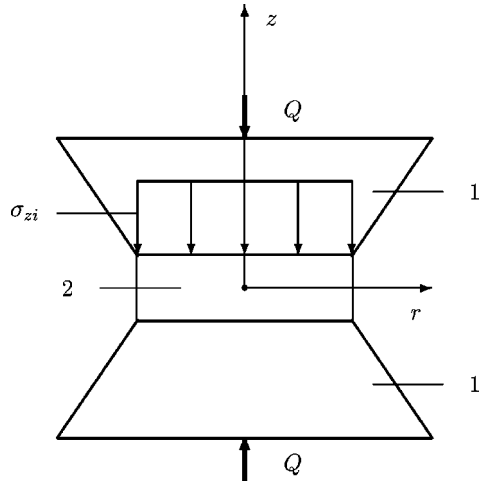

FIG. 2. Compression of materials in diamond anvils: (1) anvils and (2) compressed material.

10): interaction of a moving interface with various defects, e.g., point defects (solute and impurity atoms, and vacancies), dislocations, grain, subgrain and twin boundaries, and precipitates; emission of acoustic waves; and the Peierls barrier. We found[5,6] that $K=L\sigma_y$, where σ_y is the yield stress and L is a coefficient given for some materials in Refs. 5 and 6.

IV. PHASE TRANSFORMATION SCENARIO

We consider the following PT scenario. Before the PT, a sample is compressed elastically and stresses are distributed homogeneously (Fig. 2). During the PT, the axial load is fixed. According to Schmid's law, the compressive yield stress in the axial direction (z direction), when the c axis makes an angle of 3° with respect to the z axis, is an order of magnitude higher than the yield stress $\sigma_{y\perp}$ for the optimal orientation of the crystal. At rotation of a single crystal with respect to uniaxial stress, the yield stress varies from its maximum to the minimum values. If such a single crystal in diamond anvils is compressed in the axial direction, due to friction stresses, rotation of the anisotropy axis will occur. This will lead to a reduction of the yield stress in the direction of compression (rotational softening). After some critical reorientation, the carrying capacity (limit load) of the sample becomes smaller than the applied load and continues to reduce at further thickening. Due to such a rotational softening, dynamic compression occurs at constant force up to the thickness at which the carrying capacity of the sample becomes equal to the applied load.

In the case of perfectly plastic or hardening media and the PT in the central part of the disk, due to compressive volumetric transformation strain, the pressure in the PT region and the transformation work in Eq. (3) decrease significantly, which makes the PT condition worse; see Ref. 5 and Fig. 3(a). For the softening material described above, the decrease in thickness due to rotational plastic instability completely compensates the volume decrease due to the PT and increases the stresses in transforming region and transformation work. One more very significant contribution to the transformation work is related to stress redistribution. Plastic flow during the PT causes a significant pressure gradient from the periphery to the center (Fig. 3). Due to higher yield strength of cBN in comparison with rBN, a pressure self-multiplication effect is expected as well.[5] So pressure in the transforming region during the PT is much higher than before, which is in agreement with cracking in the anvil.

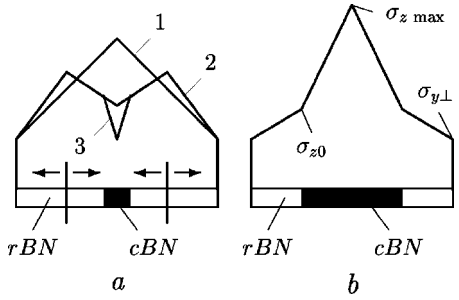

FIG. 3. (a) Axial stress distribution when material flows to the center of anvil during the PT: (1) before the PT, (2) after the PT at $\sigma_{y1}=\sigma_{y2}$, and (3) after the PT at $\sigma_{y1}<\sigma_{y2}$. (b) Axial stress distribution after the PT rBN→cBN when material flows from the center of anvil.

We conclude that a new phenomenon occurs: namely, a PT induced by rotational plastic instability. Pressure growth during the simultaneous occurrence of rotational plastic instability and the PT allows for the fulfillment of the PT criterion at significantly lower initial pressure than usually observed. We will confirm this scenario by simple estimates.

V. STRESS FIELD IN THE PROCESS OF PHASE TRANSFORMATION

We consider the initial state before the PT as a homogeneous stress state with axial stress $\sigma_{zi}=Q/\pi R^2$ (Fig. 2), where Q is the axial force which will be considered as constant during the PT. After the combination of the dynamic PT and plastic flow and reaching the equilibrium, an external ring consists of rBN with yield stress $\sigma_{y\perp}$ and internal ring is cBN with yield stress σ_{yc} [Fig. 3(b)]. We will not consider the entire deformation process, rather the final equilibrium state, and then assume that stresses vary linearly with variation of the transformation strain F_t^z during the transformation process.

We will extend our solution of the axisymmetric problem on the PT in a disk compressed in nonrotating and rotating anvils[5] for the case of large strain and anisotropic transformation strain. We employ the theory of isotropic perfectly plastic material, which can be simplified for a given problem. We will neglect the elastic deformations of anvils and deformed disk and use the well-known simplified equilibrium equation averaged over disk thickness:

$$\frac{\partial p}{\partial r}=-\frac{2\tau}{h}=-\frac{\sigma_y}{h}, \tag{4}$$

where r is the radial coordinate, h is the final thickness of the disk, τ is the shear frictional stress on the boundary S between anvils and a disk, and p is the mean (hydrostatic) pressure at the boundary S (see, e.g., Ref. 8). Equation (4)

takes into account that for a thin disk after some initial plastic flow, the shear stress τ reaches its possible maximum value $0.5\sigma_y$. Combination of this condition with the von Mises or Tresca yield conditions results in equality of all normal stresses $\sigma_z=\sigma_r=\sigma_\theta=p$ at the contact surface, which is conformed by slip line[8] and finite element[11] modeling. Using the pressure continuity condition at the boundary $r=r_0$ between rBN and cBN while solving Eq. (4), we obtain a pressure (or axial stress σ_z) distribution at the contact surface S [Fig. 3(b)]:

$$\sigma_z=\sigma_{y\perp}\left(1+\frac{R-r}{h}\right) \quad \text{at } r_0\leqslant r\leqslant R,$$
$$\sigma_z=\sigma_{z0}+\sigma_{yc}\left(\frac{r_0-r}{h}\right) \quad \text{at } r\leqslant r_0, \tag{5}$$

where

$$\sigma_{z0}=\sigma_{y\perp}\left(1+\frac{R-r_0}{h}\right)$$

is the σ_z at $r=r_0$ and boundary condition $\sigma_z=\sigma_{y\perp}$ at the external radius of anvil $r=R$ is taken into account. The applied load is determined by integration of $\sigma_z(r)$ over S:

$$Q=\pi R^2\left[\sigma_{y\perp}\left(1+\frac{R}{3h}\right)+\frac{\pi r_0^3}{3h}(\sigma_{yc}-\sigma_{y\perp})\right]=\sigma_{zi}\pi R^2, \tag{6}$$

where the equality of the applied force before and after transformation is taken into account.

VI. DETERMINATION OF PHASE TRANSFORMATION CONDITION

As we know now the stress distribution, we can evaluate the PT conditions using the PT criterion (3). For our transformation deformation gradient, the transformation work is

$$\int_{\mathbf{I}}^{\mathbf{F}_{t2}}\frac{1}{\rho}\mathbf{T}:(d\mathbf{F}_t\cdot\mathbf{F}_t^{-1})=\frac{1}{\rho^*}\mathbf{T}^*:\ln\mathbf{F}_{t2}$$
$$=\frac{1}{\rho^*}[\sigma_z^*\ln F_{t2}^z+(\sigma_r^*+\sigma_\theta^*)\ln F_{t2}^r], \tag{7}$$

where the superscript* designates some intermediate value of parameters during variation of the transformation deformation gradient from $\mathbf{I}$ to $\mathbf{F}_{t2}$. As $\ln F_{t2}^z=-0.468$, $\ln F_{t2}^r=0.020$, and $\sigma_z^*\geqslant\sigma_r^*$ and $\sigma_z^*\geqslant\sigma_\theta^*$,[8,11] then the term with $\ln F_{t2}^r$ is negligible. Neglecting F_{t2}^r, we obtain

$$\frac{1}{\rho}=\frac{1}{\rho_1}\det F_t=\frac{F_t^z}{\rho_1}$$

(as $\det F_t=V/V_1$) and

$$\int_{\mathbf{I}}^{\mathbf{F}_{t2}}\frac{1}{\rho}\mathbf{T}:(d\mathbf{F}_t\cdot\mathbf{F}_t^{-1})=\int_1^{F_{t2}^z}\frac{F_t^z}{\rho_1}\sigma_z(r)\frac{dF_t^z}{F_t^z}$$
$$=\frac{1}{\rho_1}\sigma_z^*(r)(F_{t2}^z-1). \tag{8}$$

We define $\sigma_z^*(r)$ it as a semisum of the stress before and after the PT $\sigma_z^*(r)=0.5\,[\sigma_{zi}+\sigma_z(r)]$, where $\sigma_z(r)$ is defined by Eq. (5). Substituting Eq. (8) in Eq. (3), expressing $dm_n=\rho_2 dV_{n2}$, and integrating over the final transformed volume $V_{n2}=\pi r_0^2 h$, we obtain

$$\frac{1}{m_n}\int_{m_n}\int_{\mathbf{I}}^{\mathbf{F}_{t2}}\frac{1}{\rho}\mathbf{T}:(d\mathbf{F}_t\cdot\mathbf{F}_t^{-1})dm_n$$
$$=\frac{\rho_2}{\rho_1 m_n}(F_{t2}^z-1)\int_{V_{n2}}\sigma_z^*(r)dV_{n2}$$
$$=\frac{2\pi h}{\rho_1 V_{n2}}(F_{t2}^z-1)\int_0^{r_0}\sigma_z^*(r)rdr$$
$$=\frac{1}{2\rho_1}(F_{t2}^z-1)\left(\sigma_{zi}+\sigma_{z0}+\sigma_{yc}\frac{r_0}{3h}\right)$$
$$=\frac{1}{\rho_1}\sigma_{ef}(F_{t2}^z-1). \tag{9}$$

If we compare transformation work in Eq. (9) and under the hydrostatic condition in Eq. (2), then the terms (V_2/V_1-1) and (F_{t2}^z-1) are approximately the same, and the term

$$\sigma_{ef}:=\frac{1}{2}\left(\sigma_{zi}+\sigma_{z0}+\sigma_{yc}\frac{r_0}{3h}\right), \tag{10}$$

which we will call the effective stress, plays a role similar to the PT pressure. Then we represent the final expression for the PT criterion for our problem in the following form:

$$\rho_1 X=\sigma_{ef}|F_{t2}^z-1|-a-b\,\theta=\rho_1 K. \tag{11}$$

VII. PARAMETER ESTIMATION

To quantitatively use the above theory, we need to know two material parameters σ_{yc} and $\sigma_{y\perp}$. The yield stress of cBN at compression can be estimated using the known relation $\sigma_{yc}=0.383H=19$ GPa,[8] where $H=49.6$ GPa is the hardness. Substituting this value and all parameters from the first line of Table I in Eq. (6), we obtain $\sigma_{y\perp}=0.45$ GPa.

Substituting the values of σ_{yc}, $\sigma_{y\perp}$, and all parameters from Table I in Eqs. (5), (10), and (11), we obtain the values of σ_{z0}, σ_{ef}, $\sigma_{z\,\max}$, and $\sigma_z(h)$ at $r=h$, as well as $\rho_1 K$ at $\theta=300$ K for all four cases, which are put in Table II.

Let us analyze them. During the transformation event, the axial stress in the center of the disk increases drastically to 60–76 GPa. In fact, pressure self-multiplication effect during the PT is well known at compression with shear in diamond anvils.[4,12] Such an effect was explained in Ref. 5 by the

TABLE II. Calculated values of stresses and the dissipative threshold.

	σ_{z0} (GPa)	σ_{ef} (GPa)	$\sigma_{z\,\max}$ (GPa)	$\rho_1 K$ (GPa)
1	3.05	16.50	76.13	9.70
2	2.48	13.54	59.48	8.60
3	7.31	17.54	73.81	10.09
4	4.58	15.60	67.91	9.37

increase in the yield stress and plastic flow from the center of the disk to the periphery during the PT. The pressure self-multiplication effect at compression without rotation of one anvil was not observed experimentally and contradicted existing theory.[5] The reason for such a contradiction was that in the case without rotation of the anvil, due to a volume decrease during the PT, one part of the disk material moves to the center of the anvil. Then shear stress changes sign in the central part of the disk, and according to Eq. (4), the pressure decreases at the center of the disk. The higher the yield stress of the new phase, the more the pressure decreases [Fig. 3(a)].

In this work the pressure (stress) self-multiplication effect at compression without rotation is predicted and is in agreement with a low initial PT pressure. The first reason is that the transformation compression in the axial direction is compensated for by thickness reduction due to rotational softening. The second reason is related to the anisotropic character of the transformation strain and transformational extension (rather than compression) in the radial direction. For chaotically distributed crystal orientations compression occurs in the radial direction, pressure reduces due to the PT, and higher initial pressure will be required to receive the same effective stress. As soon as both of these reasons provide complete compensation of the volume reduction due to the PT, the pressure (stress) self-multiplication effect occurs (a) due to pressure redistribution from the homogeneous one before the PT to strongly growing to the center of the disk and (b) due to the higher yield stress of cBN.

According to the PT criterion and the solution obtained, pressure growth during the PT is one of the main reasons that the PT starts at a relatively low initial pressure of 5.6 GPa. In fact, effective stress, which according to our theory affects the PT rather than initial stress, is much higher: namely, 13.54–17.54 GPa. These values are comparable with the value of pressure at which the reversible PT from rBN to cBN occurs at hydrostatic conditions.[2]

VIII. CONCLUDING REMARKS

A simple analytical model, based on a thermodynamic criterion of the PT in plastic materials and solution of the corresponding large strain plastic problem, suggests a very unexpected explanation of the low PT start pressure of 5.6 GPa of an irreversible PT of rBN→cBN. The new phenomenon—namely, a PT induced by rotational plastic instability—is revealed.

In our thermodynamic criterion, the effective stress, which is in the case under study the axial stress averaged over the transforming region and transformation process, substitutes the pressure in a classical approach. Due to drastic axial stress growth in the transforming region during the transformation process, the effective stress is of order of 13.54–17.54 GPa.

There are the following reasons for the stress increase.

(i) The main phenomenon is related to rotational plastic instability of rBN and drastic softening (reduction in the yield stress) due to reorientation of rBN crystals. This leads to a significant reduction of the disk thickness and compensates for the volume decrease due to the PT.

(ii) The second reason is related to the anisotropic character of the transformation strain and transformational extension (rather than compression) in the radial direction.

(iii) As soon as both of these reasons provide a complete compensation of the volume reduction due to the PT, the stress self-multiplication effect occurs (a) due to pressure redistribution from the homogeneous one before the PT to strongly growing to the center of the disk and (b) due to the higher yield stress of cBN.

The fact that the calculated values of the dissipative threshold $\rho_1 K$ for four very different experiments is almost the same (see Table II) strongly supports our theory. The averaged value over four experiments, $\rho_1 K = 9.44$ GPa, substituted into Eq. (11) completes this equation. Now Eqs. (5), (6), and (11) can be used to predict PT conditions, the geometry of the transformed region, and the stress distribution for various experiments.

One of the conclusions of the above analysis is that the initial pressure before the PT (5.6 GPa) does not characterize the PT conditions; it is rather the stress of the onset of rotational plastic instability. By changing initial disorientation of C axes of crystallites with respect to the compression direction and/or using some gaskets, the stress for the onset of rotational softening and, consequently, the stress when the PT starts can be changed significantly without changing the effective stress. However, there is no practical reason to reduce the σ_{zi}, because the stresses after the PT are much higher and they determine the strength and durability of diamond anvils or other types of high-pressure apparatuses which may be used for the industrial application of the effects described above. In contrast, it is necessary to increase σ_{zi}, to reduce $\sigma_{z\,\max}$ at the same effective stress, and to avoid strong dynamic instability in order to optimize the strength and durability of the loading device. The above solution in combination with the strength calculation methods and optimal design[13,14] can be used for these purposes. After finding an optimal way to produce cBN in a controlled quasistatic process without fracture of an anvil, a similar method can be applied to obtain a graphite→diamond PT, as well as to seek new superhard phases, e.g., in the B-C-N system.

It is very important that the results obtained are independent of the concrete microscopic mechanisms of the PT; i.e., they have a universal macroscopic nature. No one atomistic theory can explain the above results, because they are related to the mechanical behavior of the system of transforming particle+surrounding materials at the millimeter scale [in Eq. (5) we use geometric parameters from Table I to calculate stresses]. The continuum approach plays a supplementary role to microscopic theories and reveals new opportuni-

ties in the intensification of the PT and the production of new materials. The continuum thermomechanical methods allowed us to explain a number of experimental phenomena connected to the interaction between the PT and plasticity, in particular the effect of plastic shear strain on the PT in a diamond anvil,[5,4] some peculiarities of graphite to the diamond PT,[5] and martensite nucleation on a shear-band intersection.[15]

Even in the case of pure hydrostatic loading, shear stresses and plasticity play a very important role. It is known from theory[5,16] that even if a PT with pure volumetric transformation strain occurs in a spherical particle inside a large sphere under pure hydrostatic external pressure, nonhydrostatic stresses and plastic strain appear at a transformation strain of order of a magnitude of 0.1%–0.5%. They significantly affect PT pressure, pressure hysteresis, and transformation kinetics. Physicists may benefit significantly in the understanding and interpretation of experiments using the results of the continuum approach.

A first-principles study, which allows one to find energetic barriers and to choose the transformation path at the atomistic level,[17,18] usually uses a constant pressure (or constant volume) approximation. The stress variation in the transforming region obtained in this paper (or in Ref. 5 for hydrostatic external loading) can be used in such calculations as input data to find the transformation path for cases which correspond to more real experimental situations.

A more detailed and more microscopic finite element solution of the same problem and some additional more precise experiments to study the interaction between rotational plastic instability and the PT will be done in the near future.

ACKNOWLEDGMENTS

Discussions with Professor N. V. Novikov and Dr. I. A. Petrusha, V. V. Solozhenko, and S. B. Polotnyak are very much appreciated. Support of Texas Tech University for V.I.L. and support of the U.S. Department of State through the Science and Technology Center in Ukraine (STCU project No. 1565) for L.K.S. are gratefully acknowledged.

*FAX: (253) 679 8926. Electronic address: valery.levitas @coe.ttu.edu

[1] N. V. Novikov *et al.*, Diamond Relat. Mater. **8**, 361 (1999).
[2] M. Ueno *et al.*, Phys. Rev. B **45**, 10 226 (1992).
[3] G. J. Piermarini, S. Block, J. D. Barnett, and R. A. Forman, J. Appl. Phys. **46**, 2774 (1975).
[4] N. V. Novikov, S. B. Polotnyak, L. K. Shvedov, and V. I. Levitas, J. Superhard Mater. **3**, 39 (1999).
[5] V. I. Levitas, J. Mech. Phys. Solids **45**, 923 (1997); **45**, 1203 (1997).
[6] V. I. Levitas, Int. J. Solids Struct. **35**, 889 (1998).
[7] V. I. Levitas, Int. J. Plast. **16**, 805 (2000); **16**, 851 (2000).
[8] V. I. Levitas, *Large Deformation of Materials with Complex Rheological Properties at Normal and High Pressure* (Nova Science Publishers, New York, 1996).
[9] V. L. Solozhenko (private communication).
[10] G. Ghosh and G. B. Olson, Acta Metall. Mater. **42**, 3361 (1994).
[11] V. I. Levitas, S. B. Polotnyak, and A. V. Idesman, Strength Mater. **3**, 221 (1996).
[12] V. D. Blank *et al.*, Sov. Phys. JETP **87**, 922 (1984); V. D. Blank and S. G. Buga, Instrum. Exp. Tech. **36**, 149 (1993); V. D. Blank *et al.*, Phys. Lett. A **188**, 281 (1994).
[13] N. V. Novikov, V. I. Levitas, S. B. Polotnyak, and M. M. Potyomkin, High Press. Res. **8**, 507 (1991).
[14] N. V. Novikov, V. I. Levitas, S. B. Polotnyak, and M. M. Potyomkin, Strength Mater. **4**, 64 (1994).
[15] V. I. Levitas, A. V. Idesman, and G. B. Olson, Acta Mater. **47**, 219 (1999).
[16] A. L. Roitburd and D. E. Temkin, Sov. Phys. Solid State **28**, 432 (1986).
[17] Y. Tateyama, T. Ogitsu, K. Kusakabe, and S. Tsuneyuki, Phys. Rev. B **54**, 14 994 (1996).
[18] Y. Tateyama, T. Ogitsu, K. Kusakabe, S. Tsuneyuki, and S. Itoh, Phys. Rev. B **55**, 10 161 (1997).